OPEN

Altered Spontaneous Brain Activity in Patients With Idiopathic Trigeminal Neuralgia

A Resting-state Functional MRI Study

Jie Yuan, MD,† Song Cao, PhD,† Yue Huang, MD,* Yi Zhang, PhD,† Peng Xie, PhD,‡ Yu Zhang, PhD,‡ Bao Fu, PhD,‡ Tijiang Zhang, PhD,§ Ganjun Song, MD,§ Tian Yu, MD,‡ and Mazhong Zhang, PhD**

Objectives: To identify the changes of local coherence and intrinsic brain activity in resting-state idiopathic trigeminal neuralgia (ITN) patients by using regional homogeneity (ReHo) and fractional aptitude of low-frequency fluctuation (fALFF) analysis.

Methods: ReHo and fALFF were analyzed in 23 ITN patients and 23 age-matched and sex-matched pain-free controls to detect the functional abnormality in the brains of ITN patients. Correlations between ReHo and fALFF were analyses. ITN pain intensity were also assessed in the ITN group.

Results: Compared with pain-free controls, ITN patients exhibited significantly abnormal ReHo and fALFF in several brain regions, including the cerebellum, cingulate cortex, temporal lobe, putamen, occipital lobe, limbic lobe, precuneus, insula, medial, and superior frontal gyrus compared with healthy controls. Correlation analysis showed that ReHo values of several altered brain areas positively correlated with visual analog scale values. But no correlation was found between fALFF and visual analog scale.

Discussion: Our results showed that ITN patients exhibited significantly abnormal spontaneous brain activity in several brain regions that are involved in pain modulation and perception. The present study reflects the maladaptive process of daily pain attacks and may enhance the understanding of how chronic pain affects local intrinsic brain activity.

Key Words: trigeminal neuralgia, resting-state fMRI (rs-fMRI), chronic pain, regional homogeneity (ReHo), fractional aptitude of low-frequency fluctuation (fALFF)

(*Clin J Pain* 2018;34:600–609)

Idiopathic trigeminal neuralgia (ITN), the most prevalent disease resulting in facial pain, is characterized by paroxysmal, electric, lancinating pain sensations, and a variety of sensory experiences.[1] It is usually evoked by innocuous sensory stimuli but often occurs spontaneously. According to current opinion, ITN is supposedly caused by an ectatic blood vessel (either an artery or vein) affecting the trigeminal nerve at the root entry zone of the brain stem and secondary demyelination, probably mediated by microvascular ischemic damages.[2] The annual incidence of ITN is 0.04%, and it is estimated to affect 1 in 15,000 to 20,000 people worldwide.[3,4] Jannetta[5] first reported that 88% of his ITN patients had a nerve-vessel conflict (usually involving the superior cerebellar artery). And almost 90% of ITN patients will get pain relief after the microvascular decompression surgery, but there is no explanation why 30% of patients will experience recurrence of their pain.[6,7] Therefore, Hamlyn and King[8] proposed that a nerve-vessel conflict may represent a risk factor for the development of ITN but alone does not elicit the disease. To date, despite the prevalence of ITN and its potential medical and social burdens, the pathogenesis underlying ITN remains poorly understood.

Over the past 2 decades, accumulated neuroimaging studies have improved our understanding of how chronic pain —such as migraines, phantom limb pain, fibromyalgia, chronic back pain, and visceralgia—induces brain morphologic and functional changes in the brain's nociception modulatory areas.[9–11] Possible involvement of central components has come more and more into focus in current research, but still has an indistinct role in the pathophysiology of ITN. Several independent voxel-based morphometry studies showed gray matter (GM) changes in the bilateral superior temporal gyrus (STG)/middle temporal gyrus (MTG), thalamus, putamen, anterior and posterior insula, and primary somatosensory cortex in patients with ITN compared with the healthy controls.[12–14] Central hyperexcitability of the trigeminal system caused or sustained by peripheral mechanisms (eg, nerve-vessel conflict) was also discussed.[15,16]

However, to the best of our knowledge, very few studies have explored intrinsic brain activity alterations in individuals with ITN. Therefore, the present study was designed to determine whether changes of local coherence and intrinsic brain activity as well as associated brain regions that can become therapeutic targets, to help pain specialists relieve the suffering and improve quality of life of individuals with ITN.

Resting-state functional magnetic resonance imaging (rs-fMRI) is widely used to investigate the central mechanisms of chronic pain.[17–19] Rs-fMRI allows a shorter scanning time and provides a wide variety of results from

Received for publication July 31, 2017; revised November 9, 2017; accepted December 2, 2017.

From the *Department of Anesthesiology, Shanghai Children's Medical Center, Shanghai Jiaotong University School of Medicine, Shanghai; Departments of †Anesthesiology; §Radiology, Affiliated Hospital of Zunyi Medical College; and ‡Guizhou Key Laboratory of Anesthesia and Organ Protection, Zunyi Medical College, Zunyi, Guizhou, China.

Supported by the Shanghai Municipal Commission of Health and Family Planning, Key Developing Disciplines (grant no. 2015ZB0106), Shanghai, Chian, Pudong New District Science and Technology Development Innovation Foundation, Shanghai, China (grant no. PKJ 2013-Y61). The authors declare no conflict of interest.

Reprints: Mazhong Zhang, PhD, Department of Anesthesiology, Shanghai Children's Medical Center, 1678 Dongfang Road, Shanghai 200127, China (e-mail: shmzmzz@sina.com).

DOI: 10.1097/AJP.0000000000000578

multiple analytic approaches. Recently, data-driven methods like regional homogeneity (ReHo)[20,21] and fractional aptitude of low-frequency fluctuation (fALFF)[22] have been introduced. Data-driven methods do not need to determine a hypothesis-based seed region of interest for analysis, and they are useful for studies of symptomatic individuals without known underlying specific pathology such as our study population of ITN patients. Moreover, because it differs from the more commonly used seed-based resting-state functional connectivity analysis; the new data-driven method allows us to investigate intrinsic brain activation patterns in the whole brain.

Among the data-driven methods, ReHo was first proposed by Zang et al,[20] suggesting that ReHo exhibits superior performance compared with model-driven methods, due to its sensitivity in the detection of unpredicted and complex spontaneous hemodynamic responses in human brain function.[23] Baumgartner et al[24] used the Kendall coefficient of concordance (KCC) for purification of the activated brain clusters. On the basis of their purification work and Zang's own previous region growing method,[25] ReHo assumes that a given voxel is temporally similar to that of its neighbors. KCC was used to measure ReHo of the time series of a given voxel with those of its nearest neighbors in a voxel-wise way. Then, ReHo evaluates similarities between time series of a given voxel and its nearest neighbors, so ReHo reflects the local coherence of local spontaneous neuronal activity.[26] Specific alterations of ReHo values have been identified for the various types of chronic pain.[27–29] In contrast, the amplitude of low-frequency fluctuations (ALFF) is an index and its value is the average square root of power of spectrum, which is used to detect the regional spontaneous neuronal activity by rs-fMRI.[30] This index was subsequently used to differentiate 2 resting states, that is, eyes open versus eyes closed.[31] Moreover, ALFF has already been applied to patient studies including chronic pain,[32,33] attention deficit hyperactivity disorder,[34] and early Alzheimer disease.[35] However, it has been indicated that the ALFF is also sensitive to the physiological noise.[36] Then, a fractional ALFF (fALFF) approach was proposed. fALFF is measured by dividing the chosen low-frequency band (eg, 0.01 to 0.08 Hz) by all the frequencies measured and has proven to be more gray-matter–specific and sensitive to detect spontaneous brain activities.[22,34] The advantage of this method thus is its ability to determine the corresponding region of impairment, which may prove to be a therapeutic target in the future.

Therefore, the aim of the present study was to detect alterations in intrinsic brain activity in individuals with ITN and to use these data to identify specific brain areas that may be associated with the development and persistence of this debilitating facial pain, as well as to perform a correlation analysis between the intrinsic neural activity index and clinical variables.

METHODS

Participants

This fMRI study was approved by the ethics committee of the local hospital and informed consent was obtained from all participants. In total, 23 right-handed ITN patients were recruited from the Pain Medicine Department of this hospital between March 2016 and 2017. The diagnosis of ITN was reconfirmed in a face-to-face interview by experienced neurologists according to the International Classification of Headache Disorders (ICDH-II) criteria.[37,38] All patients had active painful attacks at time of study inclusion and all patients receive no preventative treatment before scan. The following criteria for an ITN diagnosis were used: (1) unilateral pain in the distribution of one or more branches (the ophthalmic [V1], the maxillary [V2], and the mandibular [V3]) of the trigeminal nerve; (2) stereotypical attacks with characteristic (intense, sharp, superficial, or stabbing paroxysmal) pains precipitated from trigger areas or by trigger factors for each patient; (3) no additional neurological or sensory deficits in all patients; and (4) no prior microvascular decompression surgery or other invasive treatments for ITN (ie, percutaneous radiofrequency thermocoagulation). Three patients were excluded for remarkable cerebral infarctions or head movement. Finally, data from 23 patients were analyzed: 14 men and 9 women, ranging in age from 41 to 84 years (mean, 59.6 y). In total, 23 age-matched and sex-matched right-handed pain-free volunteers (12 men and 11 women, ranging in age from 45 to 78 y, mean 63.1 y) were recruited as controls. Nineteen patients showed a nerve-vessel conflict on MRI. All participants had no head traumatic before fMRI scan. All volunteers in the control group were free from pain, brain structural abnormalities, and neuropsychiatric disorders. For demographics and participants characteristics, see Table 1.

Image Acquisition

fMRI experiments were performed using a GE Sigma HDxT 3.0-T MRI scanner (General Electric Company) with a standard 8 channel head coil. Rs-fMRI data were acquired using an echoplanar image sequence with parameters as follows: thickness/gap = 4.0/0 mm, matrix = 64×64, repetition

TABLE 1. Demographic and Clinical Characteristics of the Participants

	n = 23		
	ITN Patients	**Pain-free Controls**	***P***
Age (mean ± SEM) (y)	59.6 ± 12.5	63.1 ± 9.8	0.29 (2-sample *t* test)
Sex (male:female)	14/9	12/11	> 0.76 (χ^2 test)
Education (y)	9.4 ± 3.2	11.3 ± 4.3	0.72 (2-sample *t* test)
Duration of illness (y)	5.69 ± 3.33	NA	—
Pain location V1/V2/V3 (%)	2 (0.22)/11 (0.39)/10 (0.39)	NA	—
VAS score (mean ± SEM)	8.1 ± 1.6	NA	—
Nerve-vessel contact detected on MRI	19	NA	—

ITN indicates idiopathic trigeminal neuralgia; MRI, magnetic resonance imaging; NA, not applicable; SEM, SE of the mean; V1, ophthalmic; V2, maxillary division; V3, mandibular division; VAS, visual analog scales.

time = 2000 ms, echo time = 40 ms, flip angle = 90 degrees, field of view (FOV) = 240×240 mm. A total of 210 timepoints and 33 axial slices were obtained in 7 minutes. High-resolution anatomic 3-D T1 (repetition time = 5.8 ms, echo time = 1.8 ms, flip angle = 12 degrees, thickness/gap = 1.0/0 mm, 196 sagittal slices, FOV = 256×256 mm, matrix = 256×256) images were also acquired.

Image Processing

Preprocessing was performed using the Data Processing Assistant for Resting-State fMRI (DPARSF, http://rest.restfmri.net/forum/DPARSF)[39] and SPM8 (Wellcome Department, University College of London, UK) software based on MATLAB R2012a (MathWorks). DPARSF was used to allow for scanner calibration and participants' adaptation to the scan, so the first 10 volumes were discarded. The remaining 200 volumes were further analyzed. Processing steps included slice timing, head-motion correction, spatial normalization in the Montreal Neurological Institute space, and resampling with a $3\times3\times3\ mm^3$ resolution. Patients in pain may invariably move in the scanner; participants with head-motion >2.0 mm of translation or >2.0 degrees of rotation in any direction were excluded from further processing. The linear trend of the fMRI data was removed.

For ReHo, the band-pass filtering (0.01 to 0.08 Hz) was conducted to discard high-frequency physiological noise and the frequency drift <0.01 Hz.[40] The Resting-State fMRI Data Analysis Toolkit (REST, http://rest.restfmri.net) 1.8[41] was then used to generate individual ReHo maps by calculating the KCC of the time series of a given voxel with those of its neighbors (26 voxels) in a voxel-wise way.[20] As such, ReHo reflects the local coherence of spontaneous neuronal activity. Then a whole-brain mask was adopted to remove the nonbrain tissues. For standardization purposes, the individual ReHo maps were divided by their own global mean KCC within the whole-brain mask. Then spatial smoothing was performed on the standardized individual ReHo map with a Gaussian kernel of 4 mm full-width at half maximum.[42] fALLF represents the power or amplitude of intrinsic brain activity in a given voxel.

After the preprocessing, fALFF calculations were performed described previously.[43,44] Briefly, the resampled images were smoothed with a Gaussian kernel of 4 mm. Then the frequency band filtering was set at 0.01 to 0.08 Hz, and the time courses were converted to the frequency band using a Fast Fourier Transform. To reduce the global effects of variability across participants, each result map was respectively normalized by the global mean of the ReHo and the fALFF value.[45] The mean and SD of each individual's ReHo and fALFF values were calculated by DPARSF within the whole-brain threshold mask. *Z*-scores were then calculated in a voxel-wise way by subtracting the mean ReHo and fALFF value from each voxel's value, and then dividing by the SD of ReHo and fALFF value, respectively. In this way, the *Z*-score represents a voxel's ReHo and fALFF value in relation to all voxels in the whole brain. Therefore, the positive *Z*-score represents higher synchronicity (ReHo) or activity (fALFF) in that individual's brain. Likewise, a negative *Z*-score represents lower synchronicity or activity.[44]

Statistical Analyses

Demographic and clinical data were analyzed with Prism 6.0 (GraphPad Software Inc.). Two-sample *t* tests were used for detecting the differences in the age, visual analog scale (VAS) scores, and pain duration between ITN patients and pain-free controls. A χ^2 test was used to assess the difference in sex composition between the ITN and pain-free controls. The threshold criterion for statistical significance was $P<0.05$.

The protocol for determination of significance of ReHo and fALFF was as reported previously.[18,44] Briefly, 2-sample *t* tests were conducted in a whole-brain voxel-wise way with REST 1.8 to compare ReHo and fALFF between the ITN patients and the pin-free controls. To determine the significance of ReHo and fALFF, multiple comparison corrections were performed by Monte Carlo simulations[46] using the REST AlphaSim utility.[41] Voxels with $P<0.05$ (by 2-tailed tests, corrected by AlphaSim, rmm = 4 mm, cluster size $>1458\ mm^3$ [54 voxels]; http://afni.nih.gov/afni/docpdf/AlphaSim.pdf) were regarded as showing a significant difference between 2 groups. For correlation analysis between ReHo, fALFF, and VAS, the Pearson correlations were performed in a whole-brain voxel-wise way with REST toolbox. $P<0.05$ (2-tailed, AlphaSim corrected) again was set as the threshold for a significant difference. The REST Slice Viewer was routinely used for displaying the results[41] and generating graphs. The brain areas can be overlaid on structural brain images. A color-bar was set to illustrate the threshold.[44]

RESULTS

Comparison of ReHo Between ITN and Control Group

In comparison with the control participants, ITN patients showed significantly increased ReHo in the posterior lobe of the cerebellum, anterior cingulate and MTG, the precuneus, and the medial and superior frontal gyrus. Lower ReHo was mainly observed in the cerebellum and insula (Table 2 and Fig. 1).

Comparison of fALFF Between ITN and Control Group

In comparison with the controls, ITN patients showed increased fALFF mainly in the left and right putamen. Lower fALFF was observed in the occipital lobe (Table 3 and Fig. 2).

Correlation Between ReHo Value and VAS Score

As shown in Table 4 and Figures 3 and 4, the ReHo value of the posterior lobe of the cerebellum and the MTG were positively correlated with VAS score. Nevertheless, the ReHo value of the anterior cingulate cortex (ACC), precuneus, medial frontal gyrus, superior frontal gyrus, and insula were negatively correlated with VAS score (Table 4 and Figs. 3, 4).

Correlation Between fALFF Value and VAS Score

According to the correlation analysis, there was no significant statistical relationship between the fALFF values and the VAS score.

DISCUSSION

In this study, we evaluated abnormal local coherence and spontaneous brain activity in ITN patients using data-driven analyses, the ReHo and fALFF. Compared with pain-free controls, ITN patients showed abnormal local coherence (ReHo) and intrinsic brain activity (fALFF) in

TABLE 2. Brain Areas With ReHo Differences Between the ITN and Control Groups ($P < 0.05$, AlphaSim Corrected)

Region (R; L)	Peak MNI Coordinate			Peak *T*-value	Voxel Size	Brain Volume (mm^3)
	x	*y*	*z*			
ITN > control						
Cerebellum posterior lobe_R	57	−54	−42	3.6763	84	2268
Anterior cingulate cortex_R	15	51	30	5.2292	61	1647
Middle temporal gyrus_L	−42	−87	30	3.5438	84	2268
Precuneus_R	−6	−66	24	3.2829	141	3807
Medial frontal gyrus_L	−12	48	24	4.5206	259	6993
Superior frontal gyrus_L	−21	15	66	3.6261	83	2241
ITN < control						
Cerebellum_R	9	−48	0	−4.6973	431	11,637
Insula_L	−42	−12	6	−4.6319	133	3591

Coordinates *x*, *y*, *z* (mm) are given in standard stereotactic MNI space. All regions listed are statistically significant at $P < 0.05$, AlphaSim corrected.
ITN indicates idiopathic trigeminal neuralgia; L, left; MNI, Montreal Neurological Institute; R, right; ReHo, regional homogeneity.

many brain regions. The patterns of ReHo and fALFF alterations we found in ITN patients were comparable with what was previously described in other chronic pain conditions, and seems to reflect the cortical adaptation to long-term, highly frequent pain perceptions.[47] Significantly abnormal local coherence and spontaneous brain activity occurred in regions of the brain that are associated with pain perception and modulation. Compared with pain-free controls, ITN patients showed widely distributed ReHo alterations, such as decreased ReHo in right cerebellum and left insula and increased ReHo in the posterior lobe of the right cerebellum, as well as the right ACC, left MTG, right precuneus, left medial frontal gyrus, and left superior frontal gyrus (Table 2 and Fig. 1). Most importantly, the abnormal ReHo values of several regions were associated with self-reported pain intensity (VAS) (Table 4 and Figs. 3, 4).

Compared with pain-free controls, the ITN patients showed fALFF increases in the left and right putamen. Lower fALFF was observed mainly in the left occipital cortex and right limbic lobe (Table 3 and Fig. 2). Nevertheless, there was no significant correlation between the fALFF and VAS value according to the Pearson correlation

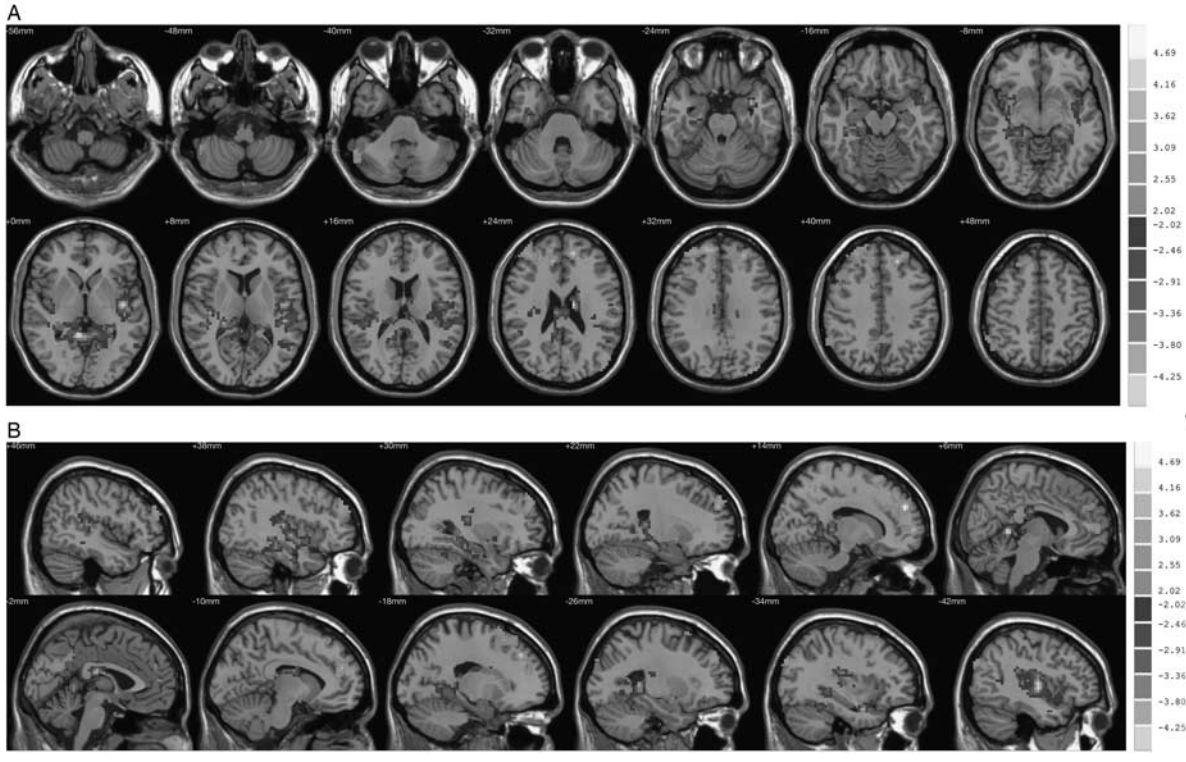

FIGURE 1. Clusters showing ReHo differences between ITN patients and pain-free controls in axial (A) and sagittal (B) slices. The cold colors indicate lower ReHo in ITN patients than healthy control group, whereas the warm colors mean vice versa ($P < 0.05$, AlphaSim corrected). Brain images are displayed in radiology convention (eg, the left in the figure represents the right side of patients' brains and vice versa). ITN indicates idiopathic trigeminal neuralgia; ReHo, regional homogeneity.

TABLE 3. Brain Areas With fALFF Differences Between the ITN and Control Groups ($P < 0.05$, Alphasim Corrected)

Region (R; L)	Peak MNI Coordinate			Peak *T*-value	Voxel Size	Brain Volume (mm^3)
	x	*y*	*z*			
ITN > control						
Putamen_R	24	6	9	4.4156	109	2943
Putamen_L	−30	−3	−6	3.9996	122	3294
ITN < control						
Occipital lobe_L	−21	−72	−6	−3.915	56	1512
Cerebellum_R	33	−54	−30	−3.0042	56	1512

Coordinates *x*, *y*, *z* (mm) are given in standard stereotactic MNI space. All regions listed are statistically significant at $P < 0.05$, AlphaSim corrected.
fALFF indicates fractional amplitude of low-frequency fluctuation; ITN, idiopathic trigeminal neuralgia; L, left; MNI, Montreal Neurological Institute; R, right.

analysis. These brain regions with abnormal activity may be important brain areas for the development and maintenance of chronic pain in general and ITN in particular. Our study underlined the impairment of local synchronization of pain perception and modulation-related brain systems that is associated with central pain processing in patients with ITN.

Our findings are in line with other functional and structural brain imaging studies on chronic facial pain. Wang et al[48] found that ReHo values were reduced in similar regions such as the cerebellum and increased in the temporal gyrus in patients with ITN. Yu et al[27] investigated 26 patients with migraine without aura and reported that they had significantly decreased ReHo values in the right rostral ACC, the prefrontal cortex (PFC), the orbitofrontal cortex, and the supplementary motor area. In structural imaging studies, Obermann et al[14] reported that GM volume was reduced in the primary somatosensory and orbitofrontal cortices, as well as the in the secondary somatosensory cortex, thalamus, insula, ACC, cerebellum, and dorsolateral PFC in patients with ITN. Li et al[13] demonstrated that the bilateral STG/MTG, bilateral parahippocampus, left ACC, caudate nucleus, right fusiform gyrus, and right cerebellum had decreased GM volume in patients with trigeminal neuralgia. Interestingly, a recent structural study demonstrated that decreased GM volume was found in the ACC and middle cingulate cortex, insula,

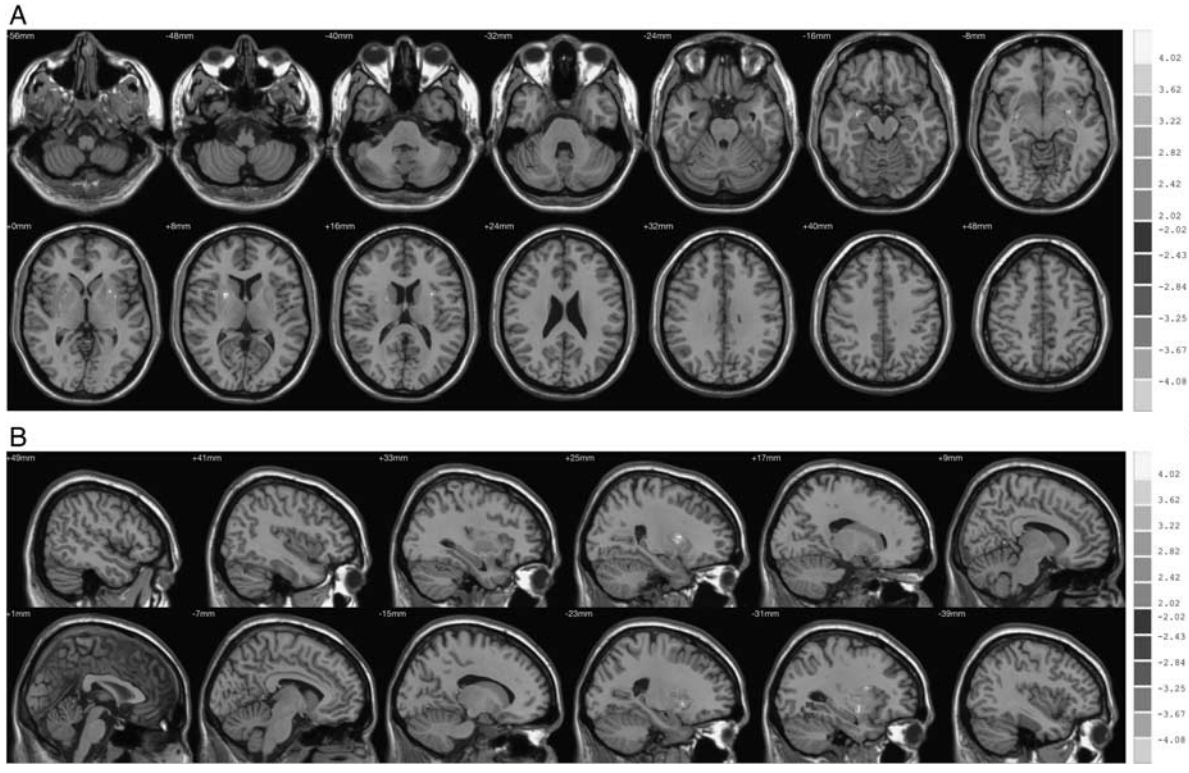

FIGURE 2. Clusters showing fALFF differences between ITN patients and pain-free controls in axial (A) and sagittal (B) slices. The cold colors indicate lower fALFF in ITN patients than pain-free control group, whereas the warm colors mean vice versa ($P < 0.05$, AlphaSim corrected). Brain images are displayed in radiology convention (eg, the left in the figure represents the right side of patients' brains and vice versa). fALFF indicates fractional amplitude of low-frequency fluctuation; ITN, idiopathic trigeminal neuralgia.

TABLE 4. Correlation Between ReHo Values and VAS Scores

Region (R; L)	Peak MNI Coordinate			Peak *R*-value	Voxel Size	Brain Volume (mm^3)
	x	*y*	*z*			
+correlation						
Cerebellum posterior lobe_R	−36	−60	−63	0.7478	319	8631
Middle temporal gyrus_L	42	6	−45	0.7193	87	2349
−correlation						
Anterior cingulate cortex_R	−3	24	33	−0.7339	57	1539
Precuneus_R	30	−78	6	−0.7033	68	1836
Medial frontal gyrus_L	39	18	21	−0.6275	56	1512
Superior frontal gyrus_L	18	9	48	−0.6166	67	1809
Insula_L	−30	21	−6	−0.6992	81	2187

Coordinates *x*, *y*, *z* (mm) are given in standard stereotactic MNI space. All regions listed are statistically significant at $P < 0.05$, AlphaSim corrected. L indicates left; MNI, Montreal Neurological Institute; R, right; ReHo, regional homogeneity; VAS, visual analog scales; +, positive; −, negative.

secondary somatosensory cortex (S2), and primary motor cortex (M1), premotor area, and several regions in the temporal lobe.[49] Although inconsistency does exist in structural and morphometric studies, the involved regions may suggest a possible neuropathology in ITN.

Cerebellum

Our results demonstrated abnormal local coherence (ReHo) and spontaneous brain activity (fALFF) in the cerebellum, and the ReHo in the posterior lobe cerebellum was positively related with VAS in participants. The cerebellum receive input from multiple cortical areas. They have been traditionally thought to modulate motor control, but are also implicated in a range of movement disorders.[50,51] Thus, altered cerebellar function may be related to impaired inhibition of the motor cortex. In contrast, the cerebellum receives extensive somatosensory input via spinocerebellar pathways, and the cerebellum may be a sensory organ.[52] Functional changes in the cerebellum could result from increased sensory input derived from long-term and high-frequency inputs associated with trigeminal neuralgia.

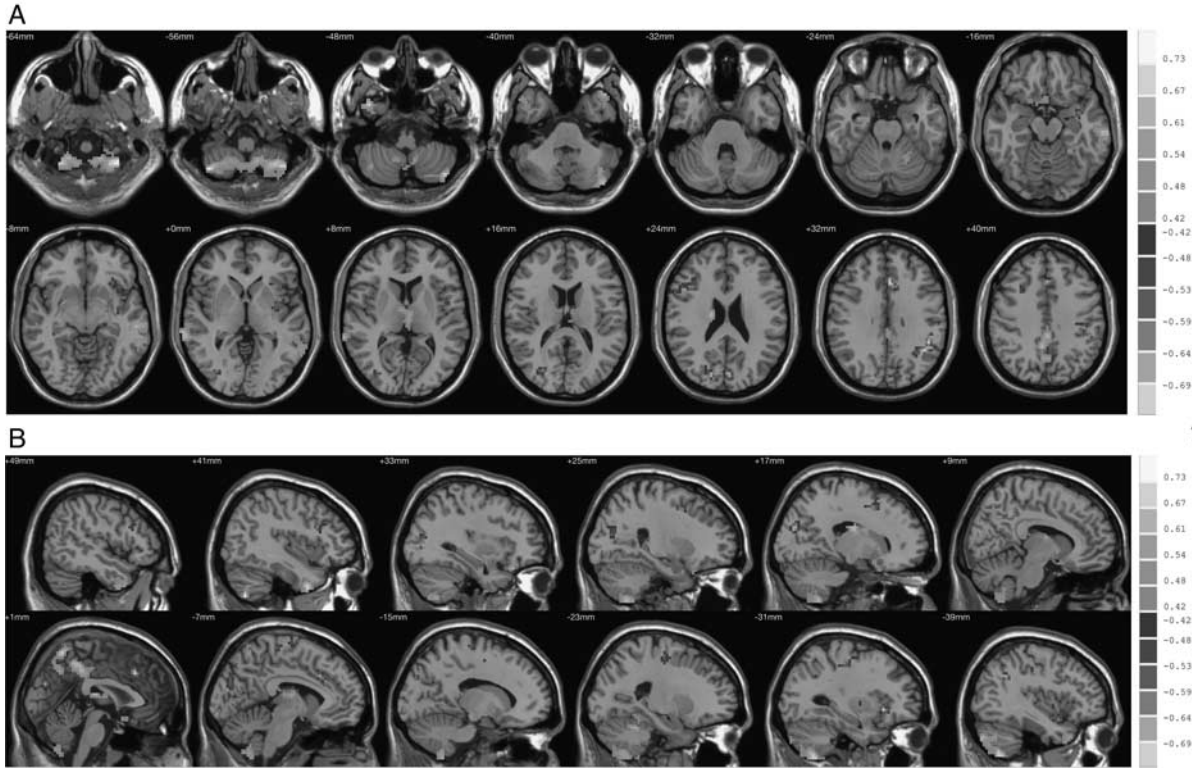

FIGURE 3. VAS value and ReHo correlation. Brain regions with colors showed significant correlation between ITN patients and pain-free controls. Their distribution is displayed in axial (A) and sagittal (B) way. The warm colors indicate higher positive correlation, whereas cool colors indicate negative correlation ($P < 0.05$, corrected). Brain images are displayed in radiology convention (eg, the left in the figure represents the right side of patients' brains and vice versa). ITN indicates idiopathic trigeminal neuralgia; ReHo, regional homogeneity; VAS, visual analog scale.

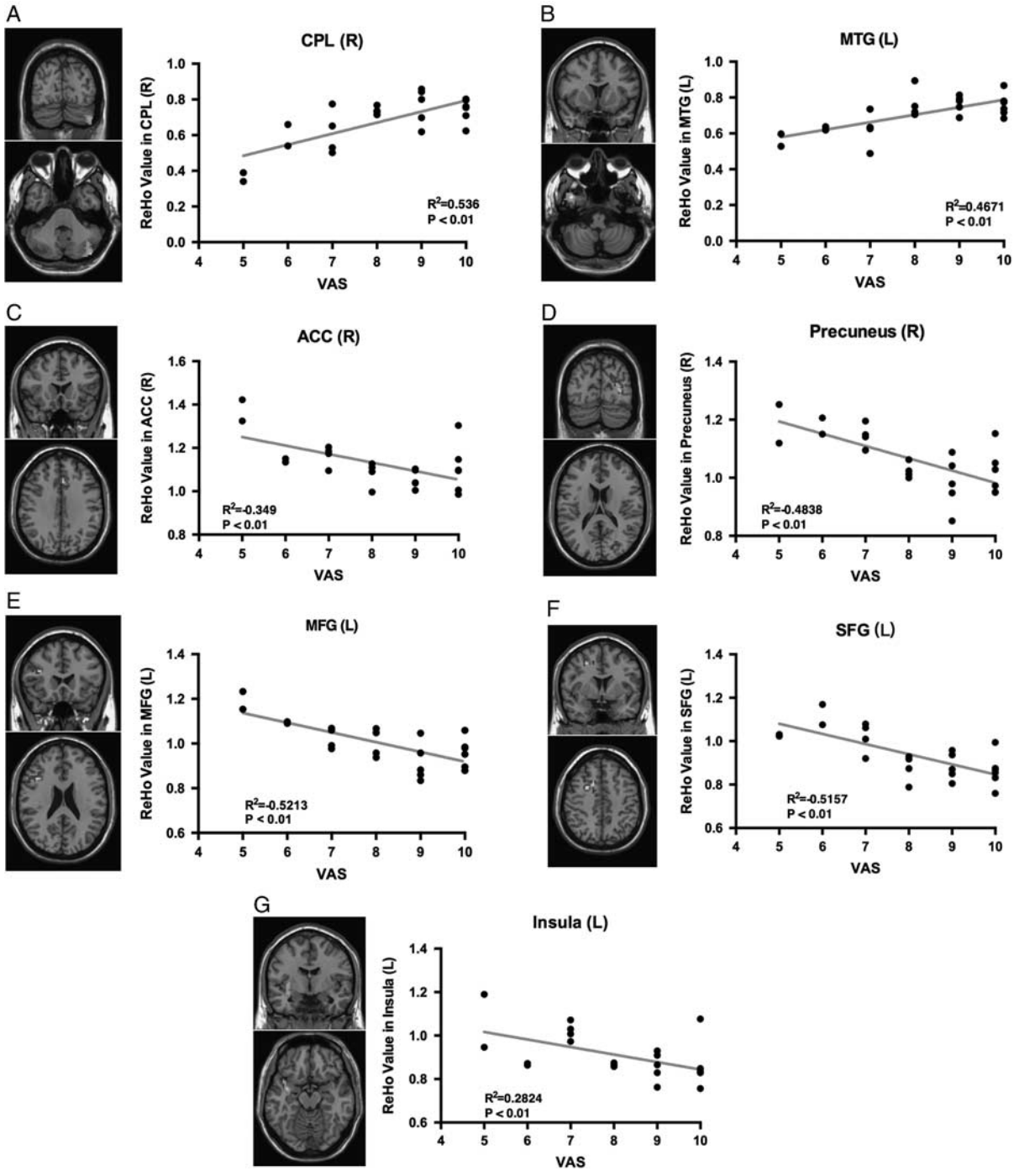

FIGURE 4. Correlation between VAS score and the ReHo values in CPL, MTG, ACC, precuneus, MFG, SFG as well as insula in the ITN patients. A, The ReHo value in CPL is positively correlates with vas in the ITN patients ($r^2 = 0.536$, $P < 0.0001$). B, The ReHo value in MTG is positively correlates with VAS in the ITN patients ($r^2 = 0.4671$, $P = 0.0003$). C, The ReHo value in ACC is inversely correlates with VAS in the ITN patients ($r^2 = -0.4671$, $P = 0.0003$). D, The ReHo value in precuneus is inversely correlates with VAS in the ITN patients ($r^2 = -0.4838$, $P = 0.0002$). E, The ReHo value in MFG is inversely correlates with VAS in the ITN patients ($r^2 = -0.5213$, $P = 0.0001$). F, The ReHo value in SFG is inversely correlates with VAS in the ITN patients ($r^2 = -0.5175$, $P = 0.0001$). G, The ReHo value in insula is inversely correlates with VAS in the ITN patients ($r^2 = -0.2824$, $P = 0.0091$). ACC indicates anterior cingulate cortex; CPL, cerebellum posterior lobe; ITN, idiopathic trigeminal neuralgia; L, left; MFG, medial frontal gyrus; MTG, middle temporal gyrus; R, right; ReHo, regional homogeneity; SFG, superior frontal gyrus; VAS, visual analog scale.

Frontal Regions

Increased ReHo in the ACC and the medial and superior frontal gyrus were detected in patients, and the ReHo was negatively correlated with VAS. The ACC was often suspected to be of paramount importance for the development of chronic pain[53,54] as a result of its integrative function on pain processing, cognition, emotion, and negative affect, all of which are associated with chronic pain or their affection pose a risk factor for the development of chronic pain, respectively.[55] A variety of cognitive processes have been shown to influence pain perception and these can specifically bias nociceptive processing in the human brain.[56] For instance, cognitive modulations of pain is usually related to activation of the prefrontal brain areas, which modulate pain perception in the cortex, including the ACC, primary somatosensory cortex (SI), secondary somatosensory cortex (SII), insula, and thalamus. This study also found reduced ReHo in the medial and superior frontal gyrus. Our previously work demonstrated that abnormal local synchronization and spontaneous brain activity were detected in the medial and superior frontal gyrus in herpes zoster and postherpetic neuralgia patients.[43,44] Higher fALFF was found in the right and left putamen in ITN group. The putamen is located at the base of the forebrain and is one of the major sites for cortical input into the basal ganglia loops.[57] The putamen is frequently activated during pain.[58] Moreover, the activity of the putamen during pain has been typically associated with the processing of pain-related motor responses.[59] Our findings indicate there may be some disruption of the PFC related to pain processing and this needs further investigation.

The Default Mode Network (DMN) and Insula

We also found that increased ReHo in the MTG and precuneus and decreased ReHo in the insula. The MTG and precuneus are parts of the DMN.[28,60] The DMN is the most stable resting-state network and is generally active when it is not engaged with any external environment.[36] The DMN is involved in mediating the recognition and rumination of pain and also can be affected by chronic pain.[61,62] Loggia et al[63] found that severe symptoms of chronic low back pain and fibromyalgia were associated with greater intrinsic DMN and DMN-insula connectivity. Moreover, patients with migraine without aura showed decreased connectivity in the prefrontal and temporal gyrus of the DMN.[64] Xue et al[65] also demonstrated that greater connectivity between the DMN and the insula is directly associated with the duration of migraine attacks. The insula cortex is another key region associated with pain processing and modulation.[66,67] The activity in the insula was increased even if someone just imagines levels of pain when looking at images of painful events (without any actual physical injuries).[68] In our present work, abnormal local coherence of the MTG, precuneus, and insula were detected in the brain scans. However, the alternations of functional connectivity between these regions and within the DMN remain to be explored.

Occipital Lobe

We observed abnormal fALFF in the occipital lobe of ITN patients. The occipital lobe is the visual processing center of the mammalian brain, containing most of the visual cortex.[69] Our previously work showed that abnormal local synchronization occurs in the occipital lobe of patients with hemifacial spasm.[18] A few ITN patients had symptoms characterized by orbital pain when the lesion was located in the ophthalmic (V1) division. We therefor can speculate that persistent orbital pain may interfere with vision. Nevertheless, the functional abnormalities detected by fALFF might be related, at least in part, to visual cortex of ITN patients. This needs further investigation.

CONCLUSIONS

In summary, we used ReHo and fALFF to detect abnormal spontaneous brain activity in ITN patients. Our results showed that ITN patients had significantly abnormalities of brain activity in the cerebellum, cingulate cortex, temporal lobe, putamen, occipital lobe, limbic lobe, precuneus, medial and superior frontal gyrus, and insula compared with healthy controls. These brain regions are mainly involved in pain modulation and perception. We also documented that pain intensity (VAS) was associated with alternative ReHo in the cerebellum, cingulate cortex, precuneus, insula, and medial and superior frontal gyrus. Our results add important information to the limited studies on brain functional alterations in patients with ITN that have been published.

Limitations

There were several limitations in the current results. First, we only focused on functional changes in ITN patients but did not examine the structural abnormalities. In the future, we will research the structural abnormalities of ITN patients' brains using voxel-based morphometry or diffusion tensor imaging analysis. Second, whether the functional changes are a consequence of the chronic pain or preexistent alterations of these regions that make patients more susceptible to the development of ITN remains unclear. Longitudinal investigations on ITN patients might help answer this question.

REFERENCES

1. Marinković S, Todorović V, Gibo H, et al. The trigeminal vasculature pathology in patients with neuralgia. *Headache*. 2007;47:1334–1339.
2. Goodwin CR, Northcutt B, Seeburg D, et al. 308° high-resolution magnetic resonance imaging findings following trigeminal rhizotomy. *Neurosurgery*. 2016;63(suppl 1):188.
3. Katusic S, Williams DB, Beard CM, et al. Epidemiology and clinical features of idiopathic trigeminal neuralgia and glossopharyngeal neuralgia: similarities and differences, Rochester, Minnesota, 1945-1984. *Neuroepidemiology*. 1991;10:276–281.
4. Mueller D, Obermann M, Yoon M-S, et al. Prevalence of trigeminal neuralgia and persistent idiopathic facial pain: a population-based study. *Cephalalgia*. 2011;31:1542–1548.
5. Jannetta PJ. Arterial compression of the trigeminal nerve at the pons in patients with trigeminal neuralgia. *J Neurosurg*. 1967;26:159–162.
6. Zakrzewska JM, Akram H. Neurosurgical interventions for the treatment of classical trigeminal neuralgia. *Cochrane Database Syst Rev*. 2011;33:CD007312.
7. Gronseth G, Cruccu G, Alksne J, et al. Practice parameter: the diagnostic evaluation and treatment of trigeminal neuralgia (an evidence-based review): report of the Quality Standards Subcommittee of the American Academy of Neurology and the European Federation of Neurological Societies. *Neurology*. 2008;71:1183–1190.
8. Hamlyn PJ, King TT. Neurovascular compression in trigeminal neuralgia: a clinical and anatomical study. *J Neurosurg*. 2009;76:948–954.
9. May A. Chronic pain may change the structure of the brain. *Pain*. 2008;137:7–15.
10. Palermo S, Benedetti F, Costa T, et al. Pain anticipation: an activation likelihood estimation meta-analysis of brain imaging studies. *Hum Brain Mapp*. 2015;36:1648–1661.

11. Simons LE, Moulton EA, Linnman C, et al. The human amygdala and pain: evidence from neuroimaging. *Hum Brain Mapp*. 2014;35:527–538.
12. Gustin SM, Peck CC, Wilcox SL, et al. Different pain, different brain: thalamic anatomy in neuropathic and non-neuropathic chronic pain syndromes. *J Neurosci*. 2011;31:5956–5964.
13. Li M, Yan J, Li S, et al. Reduced volume of gray matter in patients with trigeminal neuralgia. *Brain Imaging Behav*. 2017;11: 486–492.
14. Obermann M, Rodriguez-Raecke R, Naegel S, et al. Gray matter volume reduction reflects chronic pain in trigeminal neuralgia. *Neuroimage*. 2013;74:352–358.
15. Borsook D, Moulton EA, Pendse G, et al. Comparison of evoked vs. spontaneous tics in a patient with trigeminal neuralgia (tic doloureux). *Mol Pain*. 2007;3:34.
16. Obermann M, Yoon M-S, Ese D, et al. Impaired trigeminal nociceptive processing in patients with trigeminal neuralgia. *Neurology*. 2007;69:835–841.
17. Seminowicz DA, Labus JS, Bueller JA, et al. Regional gray matter density changes in brains of patients with irritable bowel syndrome. *Gastroenterology*. 2010;139:48.e2–57.e2.
18. Tu Y, Wei Y, Sun K, et al. Altered spontaneous brain activity in patients with hemifacial spasm: a resting-state functional MRI study. *PLoS One*. 2015;10:e0116849–10.
19. Zhang Y, Yu T, Qin B, et al. Microstructural abnormalities in gray matter of patients with postherpetic neuralgia: a diffusional kurtosis imaging study. *Pain Physician*. 2016;19: E601–E611.
20. Zang Y, Jiang T, Lu Y, et al. Regional homogeneity approach to fMRI data analysis. *Neuroimage*. 2004;22:394–400.
21. Zuo X-N, Xu T, Jiang L, et al. Toward reliable characterization of functional homogeneity in the human brain: preprocessing, scan duration, imaging resolution and computational space. *Neuroimage*. 2013;65:374–386.
22. Zou Q-H, Zhu C-Z, Yang Y, et al. An improved approach to detection of amplitude of low-frequency fluctuation (ALFF) for resting-state fMRI: fractional ALFF. *J Neurosci Methods*. 2008;172:137–141.
23. Zuo X-N, Di Martino A, Kelly C, et al. The oscillating brain: complex and reliable. *Neuroimage*. 2010;49:1432–1445.
24. Baumgartner R, Somorjai R, Summers R, et al. Assessment of cluster homogeneity in fMRI data using Kendall's coefficient of concordance. *Magn Reson Imaging*. 1999;17:1525–1532.
25. Lu Y, Jiang T, Zang Y. Region growing method for the analysis of functional MRI data. *Neuroimage*. 2003;20:455–465.
26. Wu T, Long X, Zang Y, et al. Regional homogeneity changes in patients with Parkinson's disease. *Hum Brain Mapp*. 2009;30: 1502–1510.
27. Yu D, Yuan K, Zhao L, et al. Regional homogeneity abnormalities in patients with interictal migraine without aura: a resting-state study. *NMR Biomed*. 2012;25:806–812.
28. Zhang S-S, Wu W, Liu Z-P, et al. Altered regional homogeneity in experimentally induced low back pain: a resting-state fMRI study. *J Neuroeng Rehabil*. 2014;11:115.
29. Wang P, Du H, Chen N, et al. Regional homogeneity abnormalities in patients with tension-type headache: a resting-state fMRI study. *Neurosci Bull*. 2014;30:949–955.
30. Lu H, Zuo Y, Gu H, et al. Synchronized delta oscillations correlate with the resting-state functional MRI signal. *Proc Natl Acad Sci U S A*. 2007;104:18265–18269.
31. Yang H, Long X-Y, Yang Y, et al. Amplitude of low frequency fluctuation within visual areas revealed by resting-state functional MRI. *Neuroimage*. 2007;36:144–152.
32. Zhang J, Su J, Wang M, et al. The sensorimotor network dysfunction in migraineurs without aura: a resting-state fMRI study. *J Neurol*. 2017;264:654–663.
33. Ran Q, Chen J, Li C, et al. Abnormal amplitude of low-frequency fluctuations associated with rapid-eye movement in chronic primary insomnia patients. *Oncotarget*. 2017;8:84877–84888.
34. Zang Y-F, He Y, Zhu C-Z, et al. Altered baseline brain activity in children with ADHD revealed by resting-state functional MRI. *Brain Dev*. 2007;29:83–91.
35. He Y, Wang L, Zang Y, et al. Regional coherence changes in the early stages of Alzheimer's disease: a combined structural and resting-state functional MRI study. *Neuroimage*. 2007;35: 488–500.
36. Raichle ME, MacLeod AM, Snyder AZ, et al. A default mode of brain function. *Proc Natl Acad Sci U S A*. 2001;98:676–682.
37. Benoliel R, Birman N, Eliav E, et al. The international classification of headache disorders: accurate diagnosis of orofacial pain? *Cephalalgia*. 2008;28:752–762.
38. Olesen J. The international classification of headache disorders. *Headache*. 2008;48:691–693.
39. Chao-Gan Y, Yu-Feng Z. DPARSF: A MATLAB toolbox for "Pipeline" data analysis of resting-state fMRI. *Front Syst Neurosci*. 2010;4:13.
40. Greicius MD, Krasnow B, Reiss AL, et al. Functional connectivity in the resting brain: a network analysis of the default mode hypothesis. *Proc Natl Acad Sci U S A*. 2003;100: 253–258.
41. Song X-W, Dong Z-Y, Long X-Y, et al. REST: a toolkit for resting-state functional magnetic resonance imaging data processing. *PLoS One*. 2011;6:e25031.
42. Wang L, Li K, Zhang Q, et al. Short-term effects of escitalopram on regional brain function in first-episode drug-naive patients with major depressive disorder assessed by resting-state functional magnetic resonance imaging. *Psychol Med*. 2014;44:1417–1426.
43. Cao S, Li Y, Deng W, et al. Local brain activity differences between herpes zoster and postherpetic neuralgia patients: a resting-state functional MRI study. *Pain Physician*. 2017;20: E687–E699.
44. Cao S, Song G, Zhang Y, et al. Abnormal local brain activity beyond the pain matrix in postherpetic neuralgia patients: a resting-state functional MRI study. *Pain Physician*. 2017;20: E303–E314.
45. Kim HG, Shin N-Y, Bak Y, et al. Altered intrinsic brain activity after chemotherapy in patients with gastric cancer: a preliminary study. *Eur Radiol*. 2017;27:2679–2688.
46. Ledberg A, Kerman S, Roland PE. Estimation of the probabilities of 3D clusters in functional brain images. *Neuroimage*. 1998;8:113–128.
47. Rodriguez-Raecke R, Niemeier A, Ihle K, et al. Brain gray matter decrease in chronic pain is the consequence and not the cause of pain. *J Neurosci*. 2009;29:13746–13750.
48. Wang Y, Zhang X, Guan Q, et al. Altered regional homogeneity of spontaneous brain activity in idiopathic trigeminal neuralgia. *Neuropsychiatr Dis Treat*. 2015;11:2659–2666.
49. Wang Y, Cao D-Y, Remeniuk B, et al. Altered brain structure and function associated with sensory and affective components of classic trigeminal neuralgia. *Pain*. 2017;158:1561–1570.
50. Manto M, Bower JM, Conforto AB, et al. Consensus paper: roles of the cerebellum in motor control—the diversity of ideas on cerebellar involvement in movement. *Cerebellum*. 2012;11: 457–487.
51. Calderon DP, Fremont R, Kraenzlin F. The neural substrates of rapid-onset dystonia-parkinsonism. *Nature*. 2011;14:357–365.
52. Gao JH, Parsons LM, Bower JM, et al. Cerebellum implicated in sensory acquisition and discrimination rather than motor control. *Science*. 1996;272:545–547.
53. May A. Structural brain imaging: a window into chronic pain. *Neuroscientist*. 2011;17:209–220.
54. Obermann M, Nebel K, Schumann C, et al. Gray matter changes related to chronic posttraumatic headache. *Neurology*. 2009;73:978–983.
55. Shackman AJ, Salomons TV, Slagter HA, et al. The integration of negative affect, pain and cognitive control in the cingulate cortex. *Nat Rev Neurosci*. 2011;12:154–167.
56. Quevedo AS, Coghill RC. Attentional modulation of spatial integration of pain: evidence for dynamic spatial tuning. *J Neurosci*. 2007;27:11635–11640.
57. Alexander GE, Crutcher MD. Functional architecture of basal ganglia circuits: neural substrates of parallel processing. *Trends Neurosci*. 1990;13:266–271.

58. Bingel U, Gläscher J, Weiller C, et al. Somatotopic representation of nociceptive information in the putamen: an event-related fMRI study. *Cereb Cortex*. 2004;14:1340–1345.
59. Starr CJ, Sawaki L, Wittenberg GF, et al. The contribution of the putamen to sensory aspects of pain: insights from structural connectivity and brain lesions. *Brain*. 2011;134:1987–2004.
60. Raichle ME. The brain's default mode network. *Annu Rev Neurosci*. 2015;38:433–447.
61. Kucyi A, Salomons TV, Davis KD. Mind wandering away from pain dynamically engages antinociceptive and default mode brain networks. *Proc Natl Acad Sci U S A*. 2013;110:18692–18697.
62. Kucyi A, Moayedi M, Weissman-Fogel I, et al. Enhanced medial prefrontal-default mode network functional connectivity in chronic pain and its association with pain rumination. *J Neurosci*. 2014;34:3969–3975.
63. Loggia ML, Kim J, Gollub RL, et al. Default mode network connectivity encodes clinical pain: an arterial spin labeling study. *Pain*. 2013;154:24–33.
64. Tessitore A, Russo A, Giordano A, et al. Disrupted default mode network connectivity in migraine without aura. *J Headache Pain*. 2013;14:89.
65. Xue T, Yuan K, Zhao L, et al. Intrinsic brain network abnormalities in migraines without aura revealed in resting-state fMRI. *PLoS One*. 2012;7:e52927.
66. Maleki N, Gollub RL. What have we learned from brain functional connectivity studies in migraine headache? *Headache*. 2016;56:453–461.
67. Moulton EA, Becerra L, Maleki N, et al. Painful heat reveals hyperexcitability of the temporal pole in interictal and ictal migraine states. *Cereb Cortex*. 2010;21:435–448.
68. Ogino Y, Nemoto H, Inui K, et al. Inner experience of pain: imagination of pain while viewing images showing painful events forms subjective pain representation in human brain. *Cereb Cortex*. 2007;17:1139–1146.
69. Machielsen WCM, Rombouts SARB, Barkhof F, et al. fMRI of visual encoding: reproducibility of activation. *Hum Brain Mapp*. 2000;9:156–164.

